

AN IMPROVED PERMANENT DEFORMATION MODEL  
FOR UNBOUND AGGREGATE BASE COURSE

A Thesis

by

CHARLES VANCE DRODDY

Submitted to the Office of Graduate and Professional Studies of  
Texas A&M University  
in partial fulfillment of the requirements for the degree of

MASTER OF SCIENCE

Chair of Committee,	Robert L. Lytton
Committee Members,	Edward A. Funkhouser
	Dan G. Zollinger
Head of Department,	Robin L. Autenrieth

August 2015

Major Subject: Civil Engineering

Copyright 2015 Charles Vance Droddy

## ABSTRACT

Permanent deformation of unbound base course materials under flexible pavements continue to be a significant source of the rutting observed at the surface. The permanent deformation behavior of unbound aggregate bases (UAB) has been documented by several authors. Several models have been proposed to predict the permanent deformation (rutting) occurring in the UAB. Most of the models do not take into account the stress dependent characteristics of UAB or have parameters which vary with stress state.

An improved model has been developed at Texas A&M University which includes the stress dependency in the model and this new approach has been validated. This new model incorporates power functions of the first and second invariants of the stress tensor directly in the model along with the  $\epsilon_0$ ,  $\rho$ , and  $\beta$  from existing single stage models. Several previous models attempted to achieve this by using the stress as a parameter in the fitting coefficients. This left many with relatively low values of  $R^2$  or with widely varying coefficients for a range of stress states. By using the stress state directly in the model, a generalized set of fitting parameters for a given material type have been generated. Using these generalized fitting parameters, it is shown that the new model fits the experimental data on a fundamental level.

## DEDICATION

This work is dedicated to my loving wife Mary and children Grace and Marty.  
Also to my father, Alfred Vance Droddy, who devoted his life to what you could build  
with soils.

## ACKNOWLEDGEMENTS

I would like to show my appreciation for my committee chair, Dr. Robert L. Lytton, and my committee members, Dr. Dan Zollinger, and Dr. Ed Funkhouser for their generous support and guidance throughout the course of this degree.

Thanks go to my friends and colleagues and the department faculty and staff for making my second time at Texas A&M University a great experience. Thanks also to Dr. W. Lynn Beason, Dr. Peter Keating, and Dr. Terry Kohutek for mentoring me and providing the incentive to pursue an advanced degree and keeping me focused. I would like to thank Fan Gu, Jun Zhang, and Xijun Shi for their friendship and insight in pursuit of this goal. I also want to extend my gratitude to the National Cooperative Highway Research Program, which provided funding for the research project for which this study was completed.

Finally, thanks to my family for their patience and love.

## NOMENCLATURE

AASHTO	American Association of State Highway and Transportation Officials
ASTM	American Society for Testing and Materials
LVDT	Linear Variable Differential Transformer
MEPDG	Mechanistic-Empirical Pavement Design Guide
NCHRP	National Cooperative Highway Research Program
PD	Permanent Deformation
RaTT	Rapid Triaxial Test
RLT	Repeated Load Triaxial Test
SCA	Soil Compactor Analyzer
TxDOT	Texas Department of Transportation
UAB	Unbound Aggregate Base
UGM	Unbound Granular Material
UNR	University of Nevada at Reno

## TABLE OF CONTENTS

	Page
ABSTRACT .....	ii
DEDICATION .....	iii
ACKNOWLEDGEMENTS .....	iv
NOMENCLATURE .....	v
TABLE OF CONTENTS .....	vi
LIST OF FIGURES .....	viii
LIST OF TABLES .....	x
1. INTRODUCTION .....	1
2. EXISTING MODELS .....	5
2.1 The MEPDG Model .....	5
2.2 The K-T Model .....	7
2.3 The VESYS Model .....	9
2.4 The UIUC Model .....	10
3. AN IMPROVED MODEL .....	12
4. RLT TESTING PROTOCOL .....	16
5. MATERIALS AND SPECIMEN FABRICATION .....	21
5.1 Material Properties .....	21
5.2 Specimen Fabrication .....	23
6. DETERMINATION OF MODEL COEFFICIENTS .....	26
6.1 Determination from RLT Tests .....	26
6.2 Validation .....	28

7. COMPARISON OF MODELS .....	32
8. SUMMARY AND CONCLUSIONS.....	38
REFERENCES .....	40

## LIST OF FIGURES

	Page
Figure 1 Illustration of the stress-related terms of the proposed model.....	14
Figure 2 Sensitivity of MER model to change of $I_1$ at constant $\sqrt{J_2} = 16.2$ psi .....	15
Figure 3 Sensitivity of MER model to changes of $J_2$ at constant $I_1 = 40$ psi .....	15
Figure 4 Configuration of repeated load permanent deformation test .....	17
Figure 5 LVDT's in position on load plate and RaTT cell in lowered position .....	18
Figure 6 Particle size distribution for base materials used in this study .....	22
Figure 7 Rainhart automatic compaction hammer .....	23
Figure 8 Lab measured and model predicted PD curves for granite aggregate for determination of model coefficients.....	26
Figure 9 Lab measured and model predicted PD curves for limestone aggregate for determination of model coefficients.....	27
Figure 10 Validation of prediction using the MER model for granite aggregate .....	29
Figure 11 Validation of prediction using the MER model for limestone aggregate .....	29
Figure 12 MER model correlation at 10,000 <sup>th</sup> load cycle .....	30
Figure 13 MER model correlation at 500 <sup>th</sup> load cycle .....	31
Figure 14 MEPDG model versus measured PD curves for granite aggregate .....	32
Figure 15 K-T model versus measured PD curves for granite aggregate .....	33
Figure 16 UIUC model versus measured PD curves for granite aggregate .....	33
Figure 17 MEPDG model versus measured PD curves for limestone aggregate.....	34
Figure 18 K-T model versus measured PD curves for limestone aggregate .....	34
Figure 19 UIUC model versus measured PD curves for limestone aggregate.....	35



Figure 20 Comparison of existing model accuracy at validation stress states for granite aggregate.....	37
Figure 21 Comparison of existing model accuracy at validation stress states for limestone aggregate .....	37

## LIST OF TABLES

	Page
Table 1 Proposed stress levels for calibration of model coefficients .....	18
Table 2 Proposed stress levels for validation of model coefficients .....	19
Table 3 Physical properties of base materials used in this study .....	22
Table 4 Density statistics for compacted specimens .....	24
Table 5 Post-test moisture statistics for compacted specimens.....	24
Table 6 RMSE values for model versus measured PD curves for determination of model coefficients (values in %strain).....	28

## 1. INTRODUCTION

Accumulated permanent deformation (PD) or rutting is a primary distress mechanism for unbound aggregate bases in flexible pavements. The rutting experienced in the aggregate base is typically reflected at the surface of flexible pavements. Accordingly, understanding the PD behavior of an unbound granular material (UGM) plays a significant role in the accurate evaluation and prediction of the performance of a pavement (Epps et al. 2014). In the laboratory, the PD behavior of the UGM is characterized by repeated load triaxial (RLT) tests. The responses of an unbound aggregate specimen under the repeated load include resilient (recoverable) strain and permanent (unrecoverable) strain. The recoverable behavior is characterized by the resilient modulus of the unbound aggregates (Gu et al. 2014). The permanent strain accumulated by the repeated load applications is used to describe the PD behavior (Lekarp et al. 2000). It is known that the accumulated permanent strain is mainly affected by the stress level, environmental factors, and the number of load repetitions (Tutumluer 2013, Xiao et al. 2015). Moreover, the stress induced by the traffic load is non-uniformly distributed in the base course of flexible pavements. Therefore, quantifying the effect of stress level on PD behavior of the UGM is critical to accurately predict the rutting of the unbound base layer. Unfortunately, none of the current design products consider this stress dependency in pavement performance (Tutumluer 2013).

In order to characterize the PD behavior of UGM, various rutting models have been developed to predict the accumulated PD based on number of load cycles. The

existing rutting models for UGM are generally divided into two categories, elastoplastic models and mechanistic-empirical. The rutting models of the first category are purely mechanics-based, which were developed based on elastoplastic theory (Desai 1980; Desai and Faruque 1984; Vermeer 1982; Uzan 1999; Chazallon et al. 2006; Chen et al. 2010). The advantages of these elastoplastic models are that they consider the effects of stress level and stress path on the PD of the UGM. However, they are typically complicated in analysis and time-consuming in rutting prediction, which make them difficult to be implement in pavement design. The rutting models of the second category are mechanistic-empirical models, which are focused on developing the relationship between the accumulated PD and the load repetitions (Tseng and Lytton 1989). These mechanistic-empirical models are widely used in the current pavement ME designs. They are simple in analysis, fast in computation, and provide acceptable accuracy in rutting predictions.

Based on the RLT test protocols, the mechanistic-empirical models are also categorized as two groups, including single-stage (SS) models and multi-stage (MS) models. A single-stage RLT test is performed at one stress level in one test. Multi-stage means that the RLT tests are performed at multiple stress levels in one test (Erlingsson and Rahman 2013; Gabr and Cameron 2013). The multi-stage models need to consider the effects of the stress level and the stress history on PD of the UGM, which are beyond the scope of this study. In the single stage RLT tests, multiple specimens are commonly tested at different stress levels. The most popular single-stage model is the Tseng-Lytton model (Tseng and Lytton 1989) as shown in Equation 1.

$$\varepsilon^p = \varepsilon_0^p e^{-(\frac{\rho}{N})^\beta} \quad (1)$$

Where:  $\varepsilon^p$  is the permanent strain of the granular material;

$\varepsilon_0^p$  is the maximum permanent strain;

$N$  is number of load cycles;

$\rho$  is a scale factor; and

$\beta$  is a shape factor.

$\varepsilon_0^p$ ,  $\rho$  and  $\beta$  are three unknown parameters. The Tseng-Lytton model is efficient for predicting the accumulated PD at one stress level. However, in this form, it does not consider the stress effects. Therefore, the test data from different stress levels result in different combinations of the three parameters ( $\varepsilon_0^p$ ,  $\rho$  and  $\beta$ ). In order to quantify the effect of stress level, the relationships between stress levels and the three-parameters are established based on a statistical analysis. The regression models, shown in Equations 2-4, have lower than desired R-squared values between 0.60 and 0.74 (Tseng and Lytton 1989). The regressions include the bulk stress as a weakening term which has later been shown to be incorrect (Ayres and Witczak 1998, Theyse 2002). Deviatoric stress, however, was not included in the regression models for UGM which means this method cannot accurately represent the stress dependent PD behavior in the current form.

$$\log\left(\frac{\varepsilon_0}{\varepsilon_r}\right) = 0.80978 - 0.06626W_c + 0.003077\sigma_\theta + 0.000003E_r \quad (R^2 = 0.60) \quad (2)$$

$$\log\beta = -0.9190 + 0.03105W_c + 0.001806\sigma_\theta - 0.0000015E_r \quad (R^2 = 0.74) \quad (3)$$

$$\log \rho = -1.78667 + 1.45062W_c - 0.0003784\sigma_\theta^2 - 0.0002074W_c^2\sigma_\theta - 0.0000105E_r \quad (4)$$

$$(R^2 = 0.66)$$

The objective of this study is to develop a mechanistic-empirical rutting (MER) model for UGM, which is able to predict the rutting behavior of the UGM at different stress states using the single-stage test protocol. The proposed MER model will be calibrated and validated at various confining pressures and deviatoric pressures. The developed rutting model will also be compared with existing single-stage models in terms of the rutting prediction in the RLT tests. The proposed model developed at Texas A&M University is an adaptation of the Tseng-Lytton model which incorporates a plasticity approach and uses a modified Drucker-Prager yield criterion to address incremental strains due to repeated loading (Zhang, et al. 2014).

The thesis is organized as follows. The next section presents existing models currently in use or recently developed. The following sections present the proposed MER model and the RLT test protocol. The next section describes the material properties of the aggregates used in this study. The subsequent sections calibrate and validate the proposed model then compare it with the existing models using test data from this study. The final section includes the summary and conclusions of this thesis.

## 2. EXISTING MODELS

To improve the prediction accuracy, several SS models were developed to either simplify the parameters such as the MEPDG model (ARA, 2004) or to take into account the stress effects as in the Korkiala-Tanttu (K-T) model (Korkiala-Tanttu 2009), and UIUC model (Chow et al. 2014).

### 2.1 The MEPDG Model

Currently in the United States, the most widely used model for the prediction of PD in unbound aggregate bases is a modified form of the Tseng-Lytton model which is presented as the MEPDG model (ARA, 2004). This modification was developed by Aryes under NCHRP project 1-37A in response to problems with unreasonable deformation predictions associated with non-linear stress dependent layers (Witczack – El-Basyouny, 2004). This modified model is in use in the MEPDG under AASHTO's Pavement ME software and is shown in Equation 5 which converts the plastic strain measured in the laboratory to field conditions.

$$\varepsilon_p = \beta_s \left( \frac{\varepsilon_0}{\varepsilon_r} \right) e^{-\left(\frac{\rho}{N}\right)^\beta} \varepsilon_v \quad (5)$$

Where:  $\beta, \varepsilon_0, \rho, N$  as defined above in equation 1

$\beta_s$  is a global calibration coefficient, 1.673 for granular materials

$\varepsilon_r$  is the resilient strain imposed in the laboratory test to obtain material properties; and

$\varepsilon_v$  is the average vertical resilient strain in the base layer of the flexible pavement from the response model.

$$\left(\frac{\varepsilon_0}{\varepsilon_r}\right) = \frac{\left(e^{(\rho)^\beta} \times a_1\right) + \left(e^{\left(\frac{\rho}{10^9}\right)^\beta} \times a_9\right)}{2} \quad (6)$$

$$\log \beta = -0.61119 - 0.017638\omega_c \quad (7)$$

$$\rho = 10^9 \times \left( \frac{C_0}{\left[1 - (10^9)^\beta\right]} \right)^{\frac{1}{\beta}} \quad (8)$$

$$C_0 = \ln\left(\frac{a_1}{a_9}\right) = -4.89285 \quad (9)$$

Where:

$\omega_c$  is the water content,

$a_1$  and  $a_9$  are universal constants of 0.15 and 20 respectively.

As such,  $\beta$  is estimated from a regression equation without consideration of the bulk and deviatoric stresses and  $\left(\frac{\varepsilon_0}{\varepsilon_r}\right)$  and  $\rho$  are dependent on  $\beta$  and the universal constants  $a_1$  and  $a_9$ .  $\beta$  is in turn dependent only on the water content which is



estimated in the MEPDG from the resilient modulus and the depth to the ground water table by Equation 10.

$$\omega_c = 51.712 \left[ \left( \frac{E_r}{2555} \right)^{\frac{1}{0.64}} \right]^{-0.3586 \times GWT^{0.1192}} \quad (10)$$

Where:  $E_r$  is the resilient modulus of the layer (psi)

GWT is the Ground Water Table depth (ft.)

This assumes a constant resilient modulus throughout the layer which is a source of error since it has been shown that the modulus is dependent on the stress state (Adu-Osei et al. 2001, Epps et al. 2014, Gu et al. 2014). Also, Xiao et al. in 2015 observed that high resilient modulus and thus low resilient strains did not correlate to lower permanent strains and that significant rutting could occur in high modulus granular materials. It can be seen from Equation 5 that the MEPDG model considers the effect of stress on PD by linearly projecting the plastic deformation obtained from the laboratory tests to the plastic deformation of the pavement base layer in the field by relating resilient strains (rather than stresses). The projection is an assumption without any mechanical or experimental justifications, which turns out to be inaccurate due to the nonlinear effect of the stress on the PD of the UGM.

## 2.2 The K-T Model

Equation 11 shows the K-T model developed in Finland (Korkiala-Tanttu 2009), which is widely used by researchers from Europe.

$$\varepsilon_p = C \cdot N^b \frac{R}{1-R} \quad (11)$$

$$b = d \left( \frac{q}{q_f} \right) + c' \quad (12)$$

Where:  $C$  is the permanent strain at the first loading cycle,

$N$  is the number of load cycles,

$b$  is a shear ratio parameter shown in Equation 12,

$c'$  and  $d$  are material parameters,

$$R \text{ is the shear failure ratio} = \frac{q}{q_f} = \frac{\sigma_1 - \sigma_3}{q_0 + Mp}, \quad (13)$$

$$M = \frac{6 \sin \phi}{3 - \sin \phi}, \quad (14)$$

$$q_0 = \frac{c \cdot 6 \cos \phi}{3 - \sin \phi}. \quad (15)$$

Where  $C$  and  $\phi$  are cohesion and friction angle and  $p$  is the hydrostatic stress.

The K-T model used a deviatoric shear failure ratio to capture the nonlinear effect of stress state, which is an improvement to the MEPDG model. However, limitations exist in the K-T model such as the plastic deformation goes to infinity when the load cycle goes to infinity which is unreasonable for an UGM with confinement. The use of material parameters in the computation of the shear ratio  $b$  indicate that the K-T model cannot predict the plastic deformation of the UGM at different stress levels with consistent material parameters. This model also has an inherent difficulty predicting the

deformation in the early load cycles for  $R$  values just above or below 0.5 due to the dependence on the  $C$  value.

The basis for the K-T model is a Mohr-Coulomb failure envelope. The irregular hexagonal shape of the Mohr-Coulomb yield surface leads to difficulty in analysis of stress states not aligned with the octahedral plane (Zhang et al., 2014). These issues can lead to overestimation of permanent strains at low stress levels and underestimation of permanent strains at high stress levels.

### 2.3 The VESYS Model

The VESYS model developed by W.J. Kenis (Kenis, 1978) is one of the early PD models. It determines the permanent deformation as a function of the total deflection response as shown in Equation 16.

$$R_p(n) = R_4 \left( \frac{d}{2} \right) \mu(n)^{-\alpha} \quad (16)$$

Where:  $R_p(n)$  is the permanent deformation at load cycle  $n$ ,

$R_4 \left( \frac{d}{2} \right)$  is the general deflection response,

$\mu$  and  $\alpha$  are system rutting characteristics.

The  $\mu$  system rutting characteristic represents the fractional part of the general response that becomes permanent. The  $\alpha$  is a rate term that represents the rate of change (slowing) of permanent deformation with load cycles. The characteristics are determined from the dynamic series of an Incremental Static-Dynamic test using a 10 psi

confining pressure and a deviator stress of 20 psi. It is suggested in the VESYS user guide that the system characteristics be determined at a stress state that is representative of the field conditions for the pavement location. However, most studies use the coefficients as suggested in a later calibration study by Kenis and Wang, (1997) of  $\mu$  between 0.30 – 0.50 and  $\alpha$  between 0.64 – 0.75. No subsequent studies using this model were noted that obtained the characteristics from laboratory tests for base material due to the lack of standards and difficulty at the time in running the RLT test. The VESYS model serves as the basis for the UIUC model.

## 2.4 The UIUC Model

The UIUC model (Chow et al. 2014) which is shown in Equation 17, was developed in a recent study by incorporating the power functions of deviatoric shear stress and shear strength ratio into the VESYS model.

$$\varepsilon_p = AN^B \sigma_d^C \left( \frac{\tau_f}{\tau_{\max}} \right)^D \quad (17)$$

Where:  $\sigma_d$  is the deviatoric shear stress,  $(\sigma_1 - \sigma_3)$

$N$  is the number of load cycles,

$$\tau_f \text{ is the shear stress, } = \sqrt{\left( \frac{\sigma_d}{2} \right)^2 - \left[ \sigma_f - \left( \frac{\sigma_3 + \sigma_d}{2} \right) \right]^2} \quad (18)$$

$$\tau_{\max} \text{ is the shear strength, } = c + \sigma_f \tan \phi \quad (19)$$

$\sigma_f$  is the normal stress,

$$= \frac{2\sigma_3 + 2\sigma_3 \tan^2 \phi + \sigma_d + \sigma_d \tan^2 \phi - \sqrt{\sigma_d^2 \tan^2 \phi (1 + \tan^2 \phi)}}{2(1 + \tan^2 \phi)} \quad (20)$$

$A$ ,  $B$ ,  $C$  and  $D$  are regression coefficients.

Chow (2014) conducted the RLT tests for 16 types of materials at one confining pressure (*i.e.* 5 psi) and three deviatoric stress states to validate the UIUC model. According to the test results, the UIUC model predicted the plastic deformation of the UGM with very high R-squared values. However, the four regression coefficients varied significantly from one UGM to another (*e.g.*, the coefficient  $C$  can differ greater than  $10^6$  between different UGM specimens). In addition, the study was performed at one confining pressure, thus the UIUC model still needs to be validated for the stress states at different confining pressures. More drawbacks still exist in the UIUC model, including: a) when the number of load cycles  $N$  is close to infinity, the corresponding plastic strain also goes to infinity, which is unreasonable for a confined UGM without volumetric changes; b) the model uses the shear strength ratio, which empirically assumes the contribution of shear stress to plastic strain is proportional to that of shear strength to plastic strain; c) the deviatoric shear stress term interferes with the shear strength ratio in the model, both of which represent the softening behavior of the material without addressing the hardening effect of bulk stress on the UGM.

### 3. AN IMPROVED MODEL

The new MER model, developed at Texas A&M University, given in Equation 21 is based on the original Tseng-Lytton model and includes the stress dependent effects directly. The proposed model should be able to determine the accumulation of PD for any number of load applications at a given stress state. The two terms,  $\sqrt{J_2}$  and  $\alpha I_1 + K$  are softening/ hardening terms incorporated to reflect the influence of a stress state on the PD of a UAB.

$$\varepsilon_p = \varepsilon_0 e^{-\left(\frac{\rho}{N}\right)^\beta} \left(\sqrt{J_2}\right)^m (\alpha I_1 + K)^n \quad (21)$$

$$\alpha = \frac{2 \sin \phi}{\sqrt{3}(3 - \sin \phi)} \quad (22)$$

$$K = \frac{c \cdot 6 \cos \phi}{\sqrt{3}(3 - \sin \phi)} \quad (23)$$

Where:  $J_2$  is the second invariant of the deviatoric stress tensor;

$I_1$  is the first invariant of the stress tensor;

$\varepsilon_0$ ,  $\rho$ ,  $\beta$ ,  $m$  and  $n$  are model coefficients;

$N$  is the number of load cycles,

$c$  is cohesion and,

$\phi$  is friction angle.

Figure 1 illustrates the concept of the MER model. The Drucker-Prager failure criterion (Drucker and Prager 1952), which is widely applied to rock, concrete and other pressure-dependent materials, is used in this model. As shown in Figure 1, the black dot represents the current stress state in the  $I_1 - \sqrt{J_2}$  plane.  $\sqrt{J_2}$  represents the softening effects of the deviatoric shear stress on the UGM, and a higher  $\sqrt{J_2}$  yields a larger PD. Thus the power coefficient  $m$  is always a positive number. Meanwhile, the term  $\alpha I_1 + K$  indicates the hardening/strengthening effect of the hydrostatic stress on the UGM, which is highly affected by the material cohesion and internal friction. A higher  $\alpha I_1 + K$  value results in a smaller plastic deformation, thus the power coefficient  $n$  is always a negative number. (Zhang et al. 2014; Matsuoka and Nakai 1985).

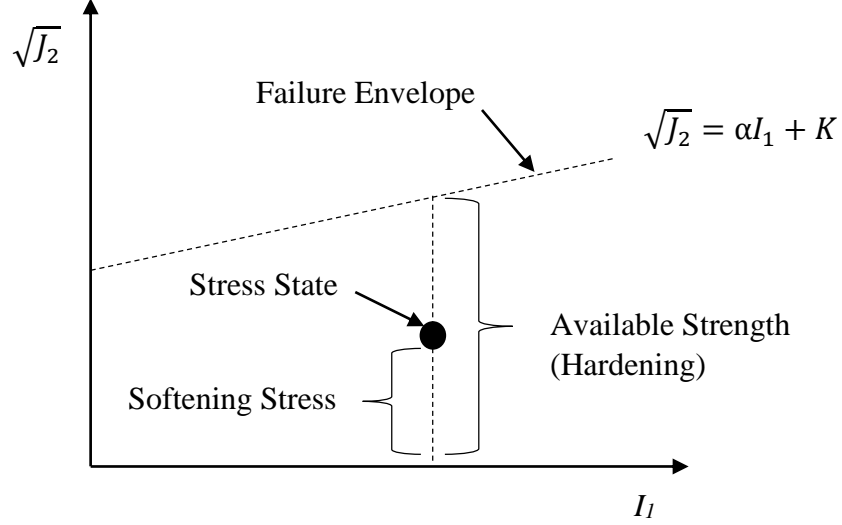


**Figure 1 Illustration of the stress-related terms of the proposed model**

The ratio of the deviatoric stress ( $\sqrt{J_2}$ ) to the stress hardening plus cohesion ( $\alpha I_1 + K$ ) determines how close to the failure envelope the stress state is which gives a measure of the plasticity of the material. The plasticity ultimately allows the material particles to rearrange into a deformed shape either by overcoming inter-particle friction or by breaking down of the particles.

The MER model is sensitive to the changes of  $I_1$  and  $\sqrt{J_2}$  as can be seen in Figure 2 and Figure 3. This sensitivity clearly shows the softening and hardening effects of the stresses in a confined volume. It also demonstrates that these stress terms are necessary for accurate prediction of PD behavior in UGM. Both stress terms are fitted well with a power function with  $R^2$  values above 0.97.



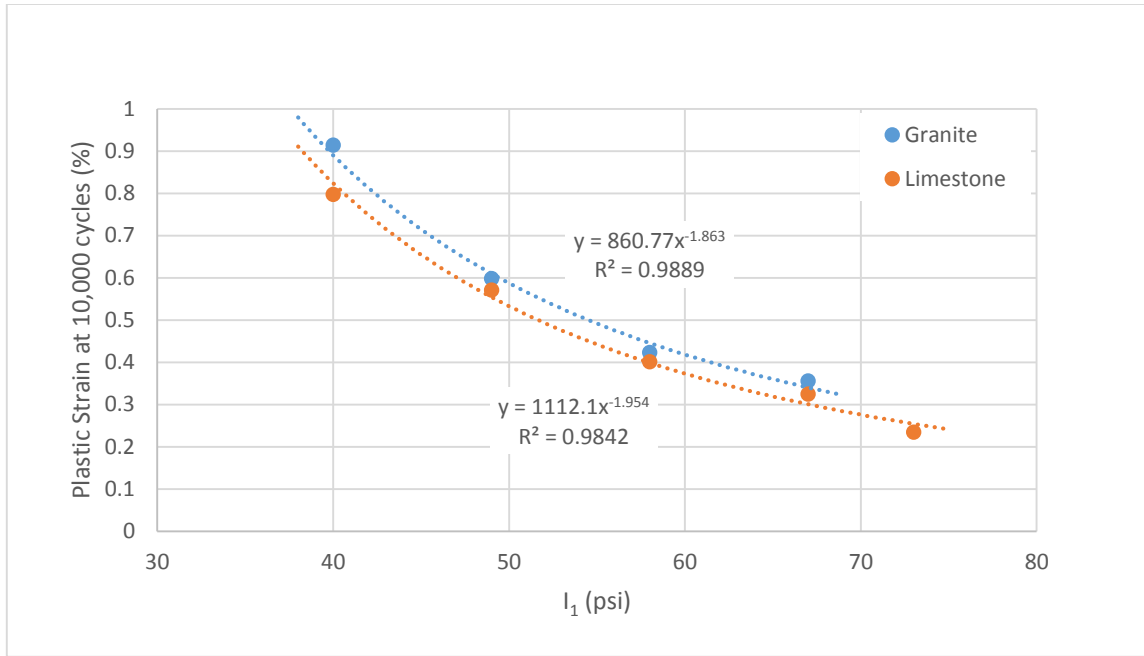


**Figure 2 Sensitivity of MER model to change of  $I_1$  at constant  $\sqrt{J_2} = 16.2$  psi**

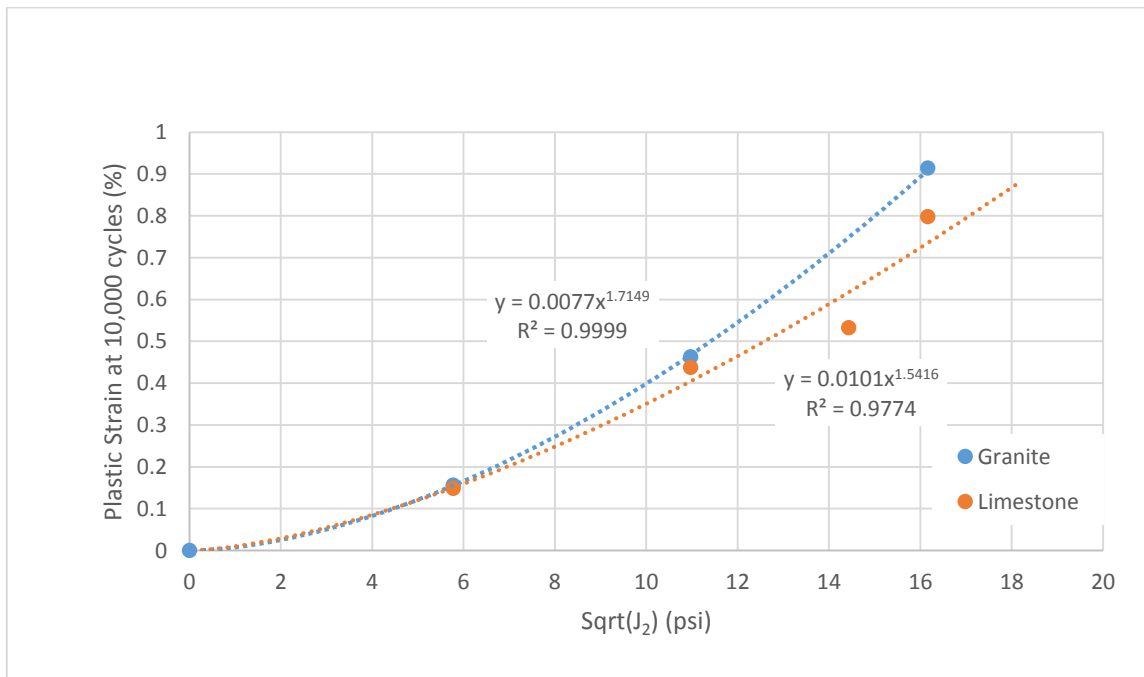


**Figure 3 Sensitivity of MER model to changes of  $J_2$  at constant  $I_1 = 40$  psi**

#### 4. RLT TESTING PROTOCOL

The RLT test is performed on cylindrical aggregate specimens using the Universal Testing Machine (UTM) with a Rapid Triaxial Test (RaTT) cell. Figure 4 shows the configuration of the RLT test. Specimens are prepared and compacted as a 6 inch diameter and approximately 6 inch tall cylinder using an automatic compaction machine with a 10 lb. hammer and 18 inch drop. Prior to testing, the RaTT cell is moved downward to encompass the specimen. A static confining pressure is applied directly to the specimen by the RaTT cell via a pneumatic bladder. The dynamic axial load is applied to the specimen through the loading frame of the UTM. The axial load follows a haversine shape with 0.1 second load period and 0.9 second rest period. In pre-conditioning, the confining pressure is controlled constantly at 15 psi (103.4 kPa), and a 15 psi (103.4 kPa) deviatoric axial load is applied for 500 repetitions (AASHTO T-307 2012). A specimen is then subjected to 10,000 cycles of repeated load at one specified stress level as shown in Table 1. During each test, two Linear Variable Differential Transformers (LVDTs) mounted on the top of the specimen are used to measure the vertical deformation of the specimen as shown in Figure 5. The test data are used to determine the PD behavior of the UGM.

Two critical steps are involved in using Equation 21 to determine the coefficients of the proposed rutting model:

- Determine the cohesion  $c$  and friction angle  $\phi$  from the triaxial compressive strength tests (TxDOT, 2010);

- Determine the coefficients  $\varepsilon_0$ ,  $\rho$ ,  $\beta$ ,  $m$  and  $n$  from the RLT tests at multiple stress levels.

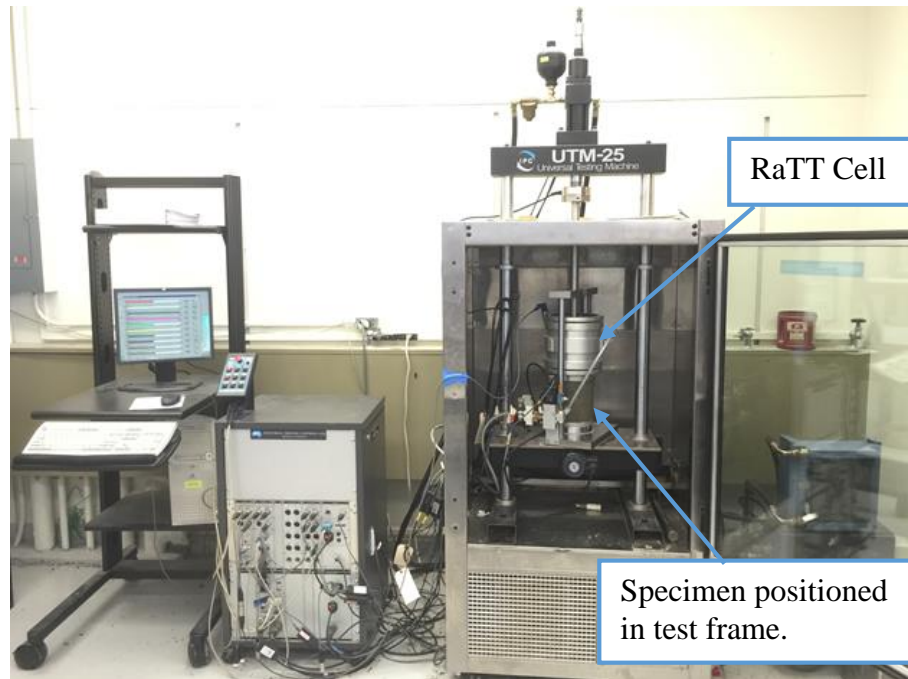


**Figure 4 Configuration of repeated load permanent deformation test**



**Figure 5 LVDT's in position on load plate and RaTT cell in lowered position**

**Table 1 Proposed stress levels for calibration of model coefficients**

<b>Stress State</b>	<b>Confining Pressure, <math>\sigma_3</math> (psi)</b>	<b>Deviatoric Stress, <math>\sigma_d</math> (psi)</b>	<b>Bulk Stress, <math>I_1</math> (psi)</b>	<b>Second Invariant of Shear Stress Tensor, <math>J_2</math> (psi<sup>2</sup>)</b>
1	4	28	40	261.33
2	7	19	40	120.33
3	10	10	40	33.33
4	13.33	0	40	0
5	7	28	49	261.33
6	10	28	58	261.33
7	13	28	67	261.33

**Table 2 Proposed stress levels for validation of model coefficients**

<b>Stress State</b>	<b>Confining Pressure, <math>\sigma_3</math> (psi)</b>	<b>Deviatoric Stress, <math>\sigma_d</math> (psi)</b>	<b>Bulk Stress, <math>I_1</math> (psi)</b>	<b>Second Invariant of Shear Stress Tensor, <math>J_2</math> (psi<sup>2</sup>)</b>
8	5	25	40	208.33
9	15	28	73	261.33

As seen in Table 1, a total of 7 stress levels are designed to determine the coefficients of the proposed rutting model. Stress states 1, 2, 3 and 4 employ the same  $I_1$  but different  $J_2$ , whereas stress states 1, 5, 6 and 7 apply the same  $J_2$  with various  $I_1$ . This test protocol allows for the quantification of the influence of  $I_1$  and  $J_2$  on the PD behavior of UGM, individually. Note that stress state 4 represents a hydrostatic state, which can also be used to verify that the plastic behavior of UGM is marginal under the hydrostatic condition. Testing of the hydrostatic stress state also demonstrates why stress state must be included in any PD model since there is no appreciable deformation at any number of load cycles.

Table 2 presents the other two stress states used to validate the determined coefficients in the proposed MER model. These stress states were chosen based on the desire to have one validation stress state within the range used for determination of model parameters and the other stress state outside the range. The use of one of the

validation states outside the parameter range shows that the model can be used to extend the useful range of the model above or below the typical testing ranges.

## 5. MATERIALS AND SPECIMEN FABRICATION

### 5.1 Material Properties

The materials used in the testing were provided from the University of Nevada at Reno (UNR) and from the TxDOT Paris District. The material provided by UNR is a granitic well graded crushed base course material with low plasticity fines. The modified effort maximum density and optimum moisture (ASTM D1557 2012) for this material are 138.7 lb/ft<sup>3</sup> at 6.7%. The material provided by TxDOT is a calcareous limestone conglomerate. The fines of this material are non-plastic and the Soil Compactor Analyzer (SCA) (TxDOT 2011) maximum density and optimum moisture are 120.5 lb/ft<sup>3</sup> at 13.5%. These materials are representative of common base course materials that are relatively well graded and are currently in use as base course in many pavements. Figure 6 shows the aggregate gradation for the two selected materials.

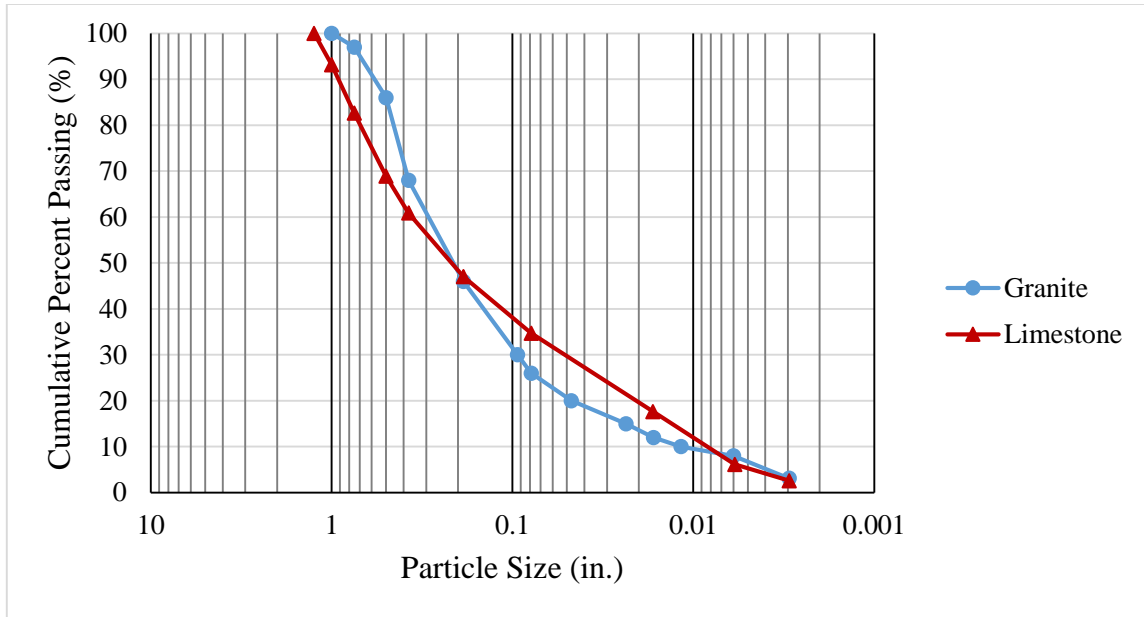


**Figure 6 Particle size distribution for base materials used in this study**

**Table 3 Physical properties of base materials used in this study**

Aggregate Type	$\gamma_d$ (lb/ft <sup>3</sup> )	$\omega$ (%)	LL	PI	c (psi)	$\Phi$ (degree)	MBV (mg/g)
Granite	138.7	6.7	25	4	2.9	51.3	6.41
Limestone	120.5	13.5	NA	NP	9.6	54.9	4.70

Table 3 lists the physical properties of the unbound aggregates, including maximum dry density  $\gamma_d$ , optimum moisture content  $\omega$ , liquid limit (LL), plasticity index (PI), cohesion  $c$ , friction angle  $\Phi$ , and methylene blue value (MBV). The presented cohesion and friction angle values will be used to determine the coefficients of the proposed rutting model.



## 5.2 Specimen Fabrication

The fabrication of specimens was completed in a manner which attempted to reduce variation between specimens. The use of the Rainhart automatic hammer shown in Figure 7 for compaction of the specimens was helpful to provide a consistent compactive effort between samples.



**Figure 7 Rainhart automatic compaction hammer**

Samples were blended to meet the gradation described in Figure 6 from previously sieved oven dry material. Then water was added to achieve optimum moisture content. The sample was then covered with aluminum foil to prevent moisture loss and allowed to slake overnight to provide time for the moisture to become more

uniformly distributed within the aggregate particles. Compaction proceeded in 4 layers to achieve specimens approximately 6 inches in height with a volume nearly 0.10 cubic foot. The ASTM D1557 modified compactive effort of 56,000 ft-lbf/ft<sup>3</sup> required 92 blows per layer. The SCA compactive effort of 23,000 ft-lbf/ft<sup>3</sup> was achieved with 38 blows per layer. Average density and moisture content for each material as tested are presented in Table 4 and Table 5.

**Table 4 Density statistics for compacted specimens**

	<b>Average density (lb/ft<sup>3</sup>)</b>	<b>Variance</b>	<b>Standard Deviation</b>	<b>Median</b>	<b>Range</b>
<b>Granite</b>	138.4	0.16	0.40	138.2	0.9
<b>Limestone</b>	114.5	0.77	0.88	114.5	2.4

**Table 5 Post-test moisture statistics for compacted specimens**

	<b>Average Moisture (%)</b>	<b>Variance</b>	<b>Standard Deviation</b>	<b>Median</b>	<b>Range</b>
<b>Granite</b>	6.26	2.76E-06	0.17	6.30	0.41
<b>Limestone</b>	13.78	4.06E-06	0.20	13.79	0.63

As seen in the tables, control of the moisture in the specimens was acceptable with less than +/- 1.0% range and less than 0.4% standard deviation per ASTM D1557. The density control for the granite was excellent with a range of only 0.9 lb/ft<sup>3</sup> and standard deviation of 0.4 lb/ft<sup>3</sup>. The limestone density was less than ideal with a range

of 2.4 lb/ft<sup>3</sup>. Acceptable single operator standard deviation and range for the density are 0.6 and 1.8 lb/ft<sup>3</sup> respectively according to ASTM D1557. It is unknown if this increased variation is due to problems with the automatic compactor during the time between testing of the granite and the limestone or due to the limited number of blows per layer using the SCA compactive effort.

## 6. DETERMINATION OF MODEL COEFFICIENTS

### 6.1 Determination from RLT Tests

Based on the results of the RLT tests, the coefficients of the MER model are determined by using the solver function in Microsoft Excel to fit the measured PD curves. The best fit was accomplished by minimizing the sum of squared errors between the predicted values and the measured values for all 7 stress states. Figure 8 and 9 present comparisons of laboratory-measured and model-predicted accumulated permanent strains at different stress levels for both granite aggregates and limestone aggregates. Stress state is abbreviated as “S” shown in the legend. The recorded permanent strain starts from the 15th load cycle.

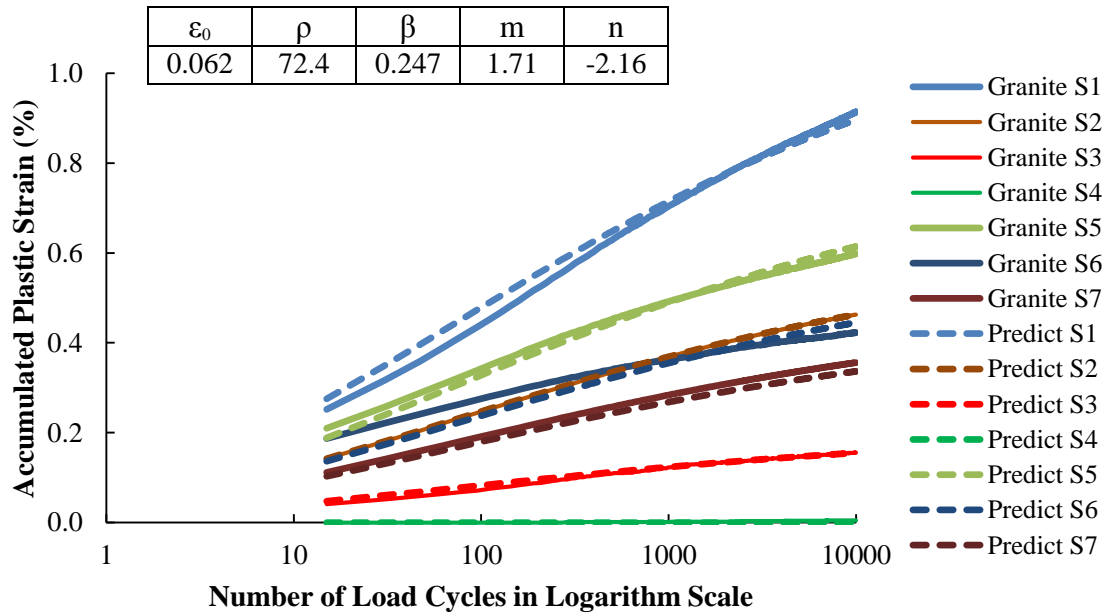


**Figure 8 Lab measured and model predicted PD curves for granite aggregate for determination of model coefficients**

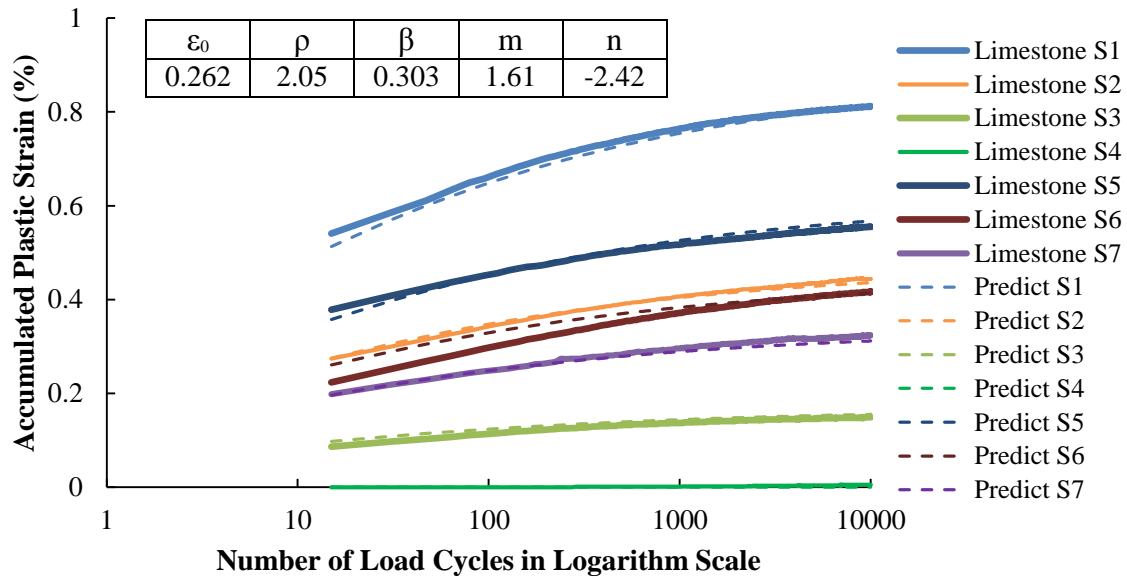


**Figure 9 Lab measured and model predicted PD curves for limestone aggregate for determination of model coefficients**

The Root Mean Squared Error (RMSE) values are calculated to evaluate the goodness of model fitting at various stress states and are shown in Table 6. It is seen that the determined RMSE in % strain at each stress level is quite small (less than 0.02%), which indicates that the MER model accurately captures the trend of the measured PD curves for both of the tested UGMs. No PD is observed in the hydrostatic stress state 4 for both of the tested materials. The use of the hydrostatic state shows that models without the stress state included will not adequately be able to predict this case due to the dependence on number of load cycles. Figure 8 and 9 also show the determined coefficients of the MER model, which can be used to predict the rutting behavior of the tested UGMs at any stress levels and number of load repetitions.

Furthermore, the positive  $m$  value indicates the softening effect of  $J_2$  and the negative  $n$  value indicates the hardening effect of  $I_1$  on the PD behavior of the UGM.

**Table 6 RMSE values for model versus measured PD curves for determination of model coefficients (values in %strain)**

Stress State	1	2	3	4	5	6	7
Granite	0.012	0.001	0.002	0.002	0.012	0.016	0.018
Limestone	0.005	0.005	0.006	0.002	0.004	0.012	0.006

## 6.2 Validation

Test data from stress states 8 and 9 shown in Table 2 are used to validate the prediction accuracy of the rutting models. Figure 10 and Figure 11 compare the measured PD curves to the MER model-predicted PD curves for both granite aggregates and limestone aggregates by using the determined coefficients shown in Figure 8 and Figure 9, respectively. It is seen that the MER model predictions have small RMSE values for the UGMs at the two stress states. These small RMSE values indicate that the model is valid for stress states within the zone of calibration and can be extended outside the zone of calibration.

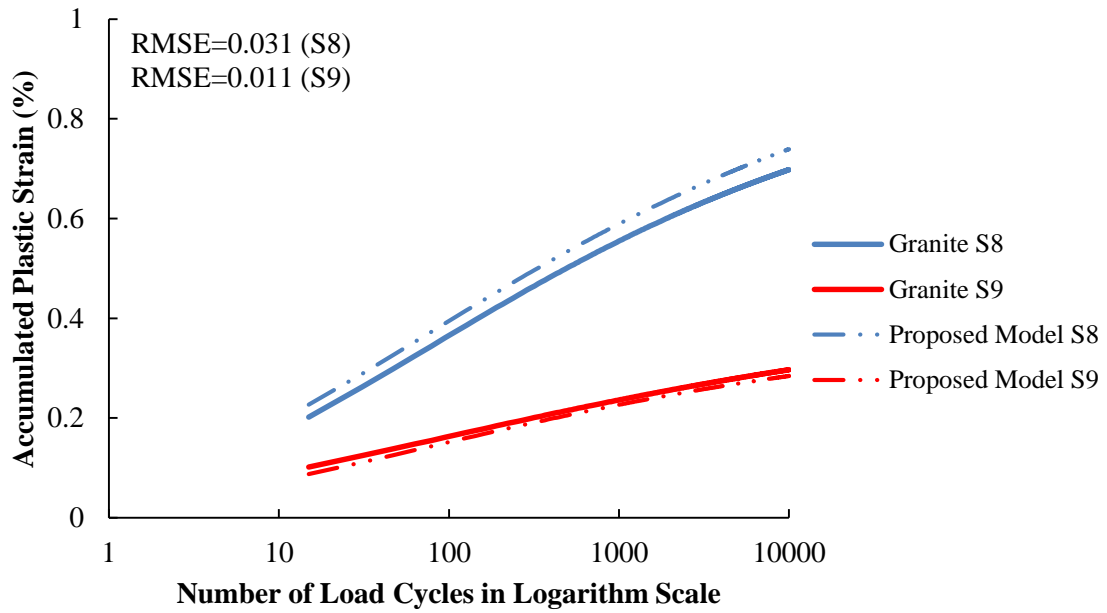


**Figure 10 Validation of prediction using the MER model for granite aggregate**

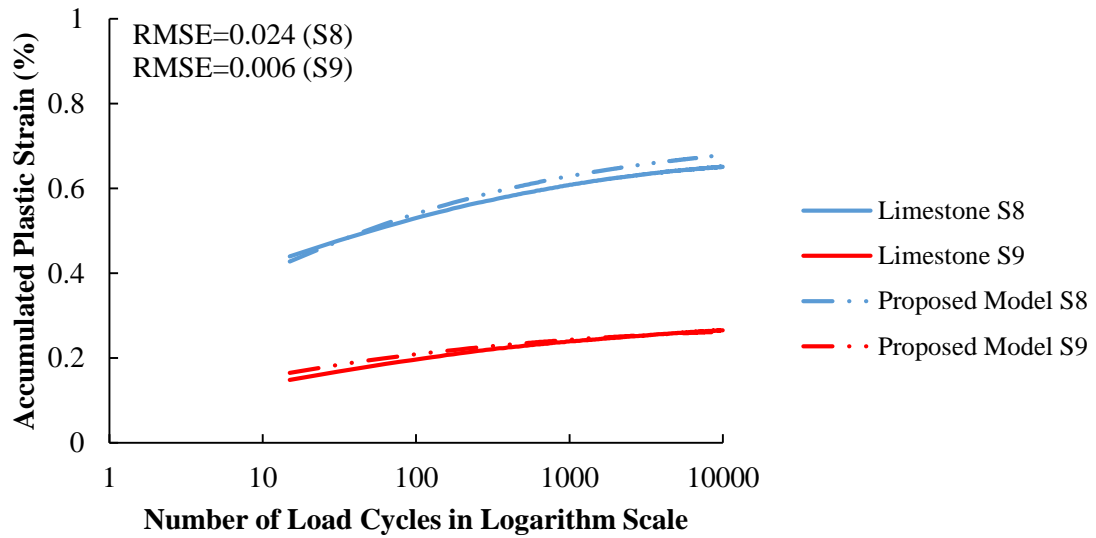


**Figure 11 Validation of prediction using the MER model for limestone aggregate**

The model accuracy for all stress states at the 10,000<sup>th</sup> load cycle can be seen in Figure 12 with an  $R^2$  of 0.9898 which shows that the MER model can accurately predict the PD at a wide range of stress states with a single set of fitting parameters. In addition, Figure 13 shows the model correlation at the 500<sup>th</sup> load cycle with an  $R^2$  of 0.9969 which indicates that the model is accurate at both the primary and secondary ranges of load cycles. Many models tend to be accurate at the final tested load cycles but cannot adequately capture the early trend in the primary range.

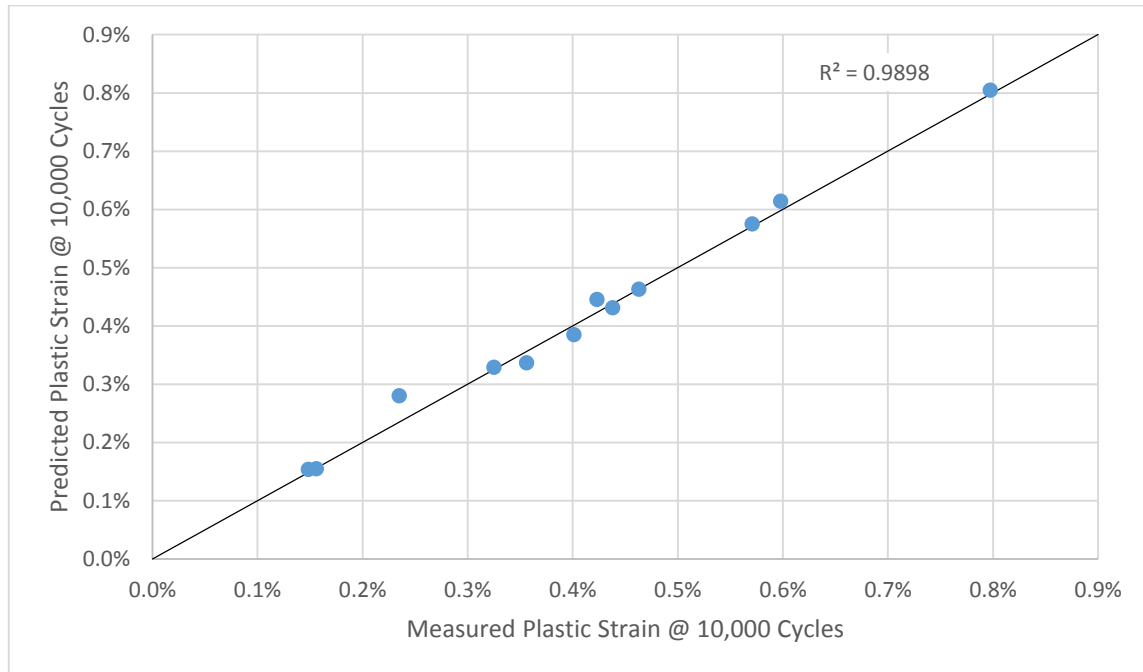


**Figure 12 MER model correlation at 10,000<sup>th</sup> load cycle**



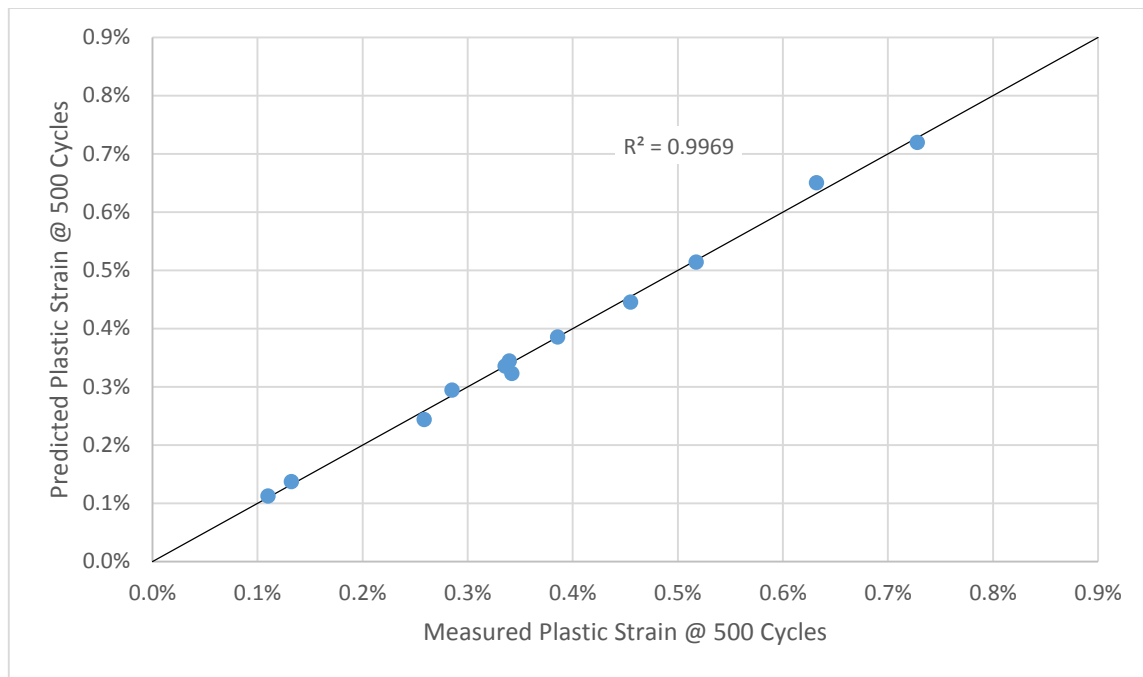


**Figure 13 MER model correlation at 500<sup>th</sup> load cycle**

## 7. COMPARISON OF MODELS

Using the same regression method and solver function, the coefficients of the MEPDG model, K-T model and UIUC model are also determined based on the RLT test data. Figure 14 thru Figure 19 compare the calibrated model predictions with the measured PD at various stress states for both the granite aggregate and limestone aggregate.

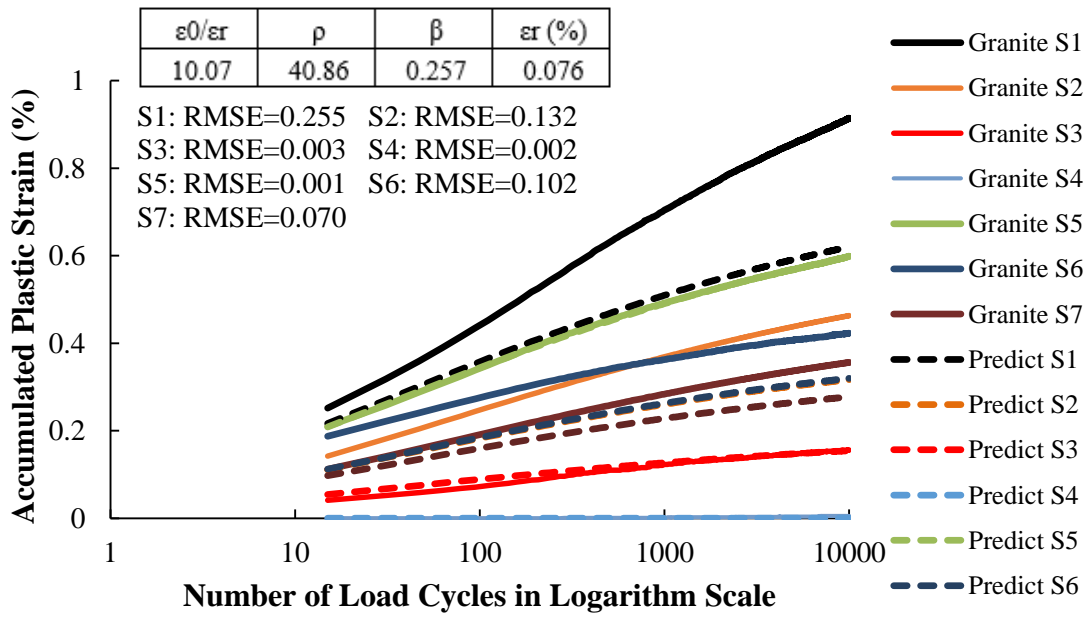


**Figure 14 MEPDG model versus measured PD curves for granite aggregate**

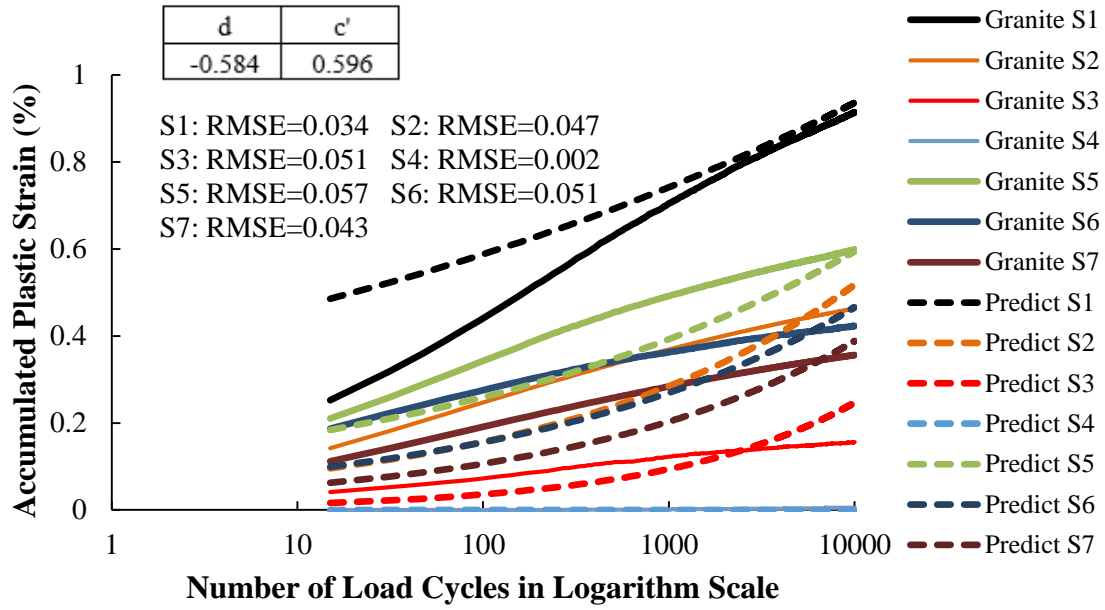


**Figure 15 K-T model versus measured PD curves for granite aggregate**

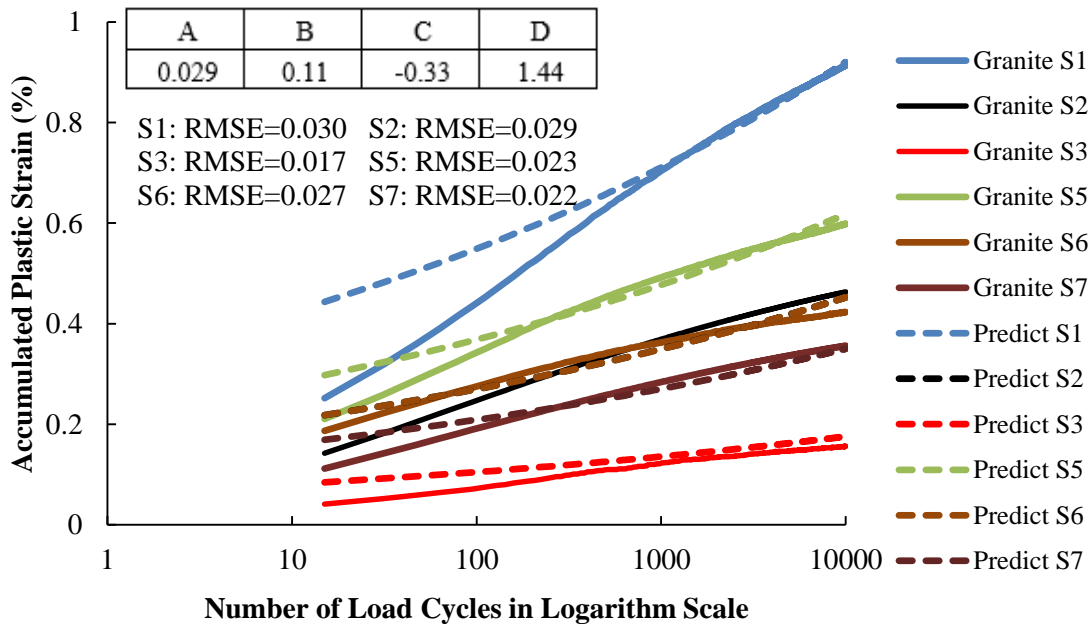


**Figure 16 UIUC model versus measured PD curves for granite aggregate**

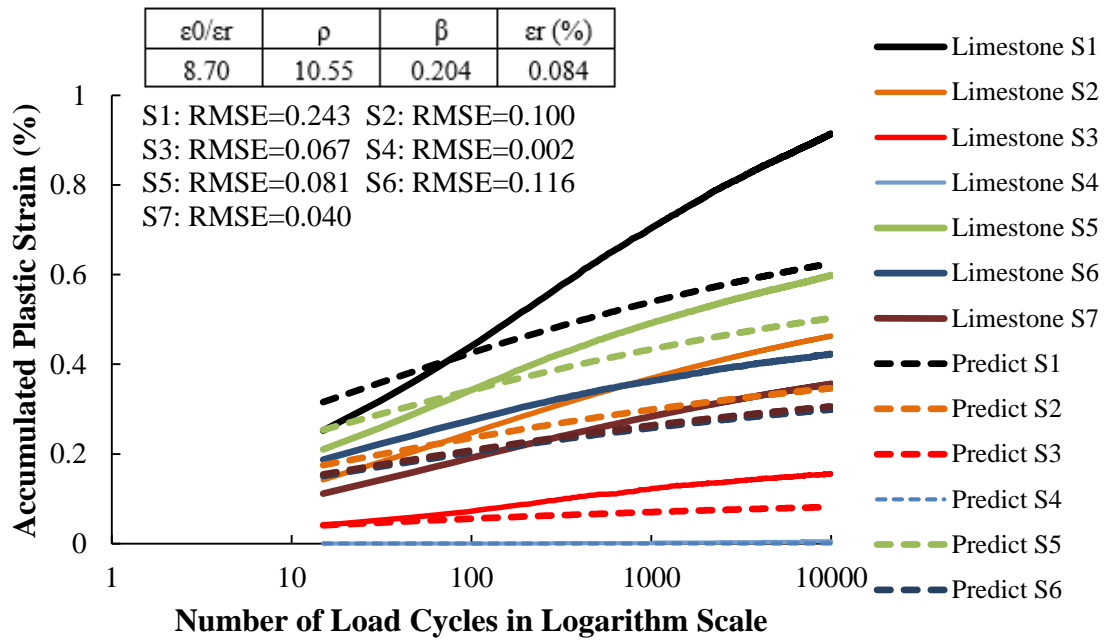


**Figure 17 MEPDG model versus measured PD curves for limestone aggregate**

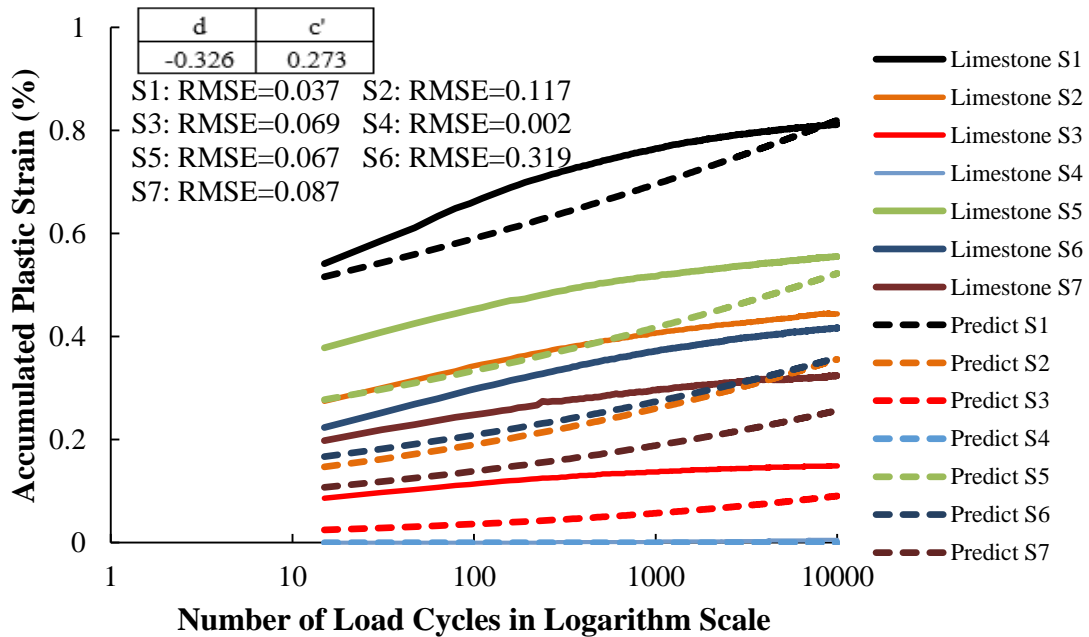


**Figure 18 K-T model versus measured PD curves for limestone aggregate**

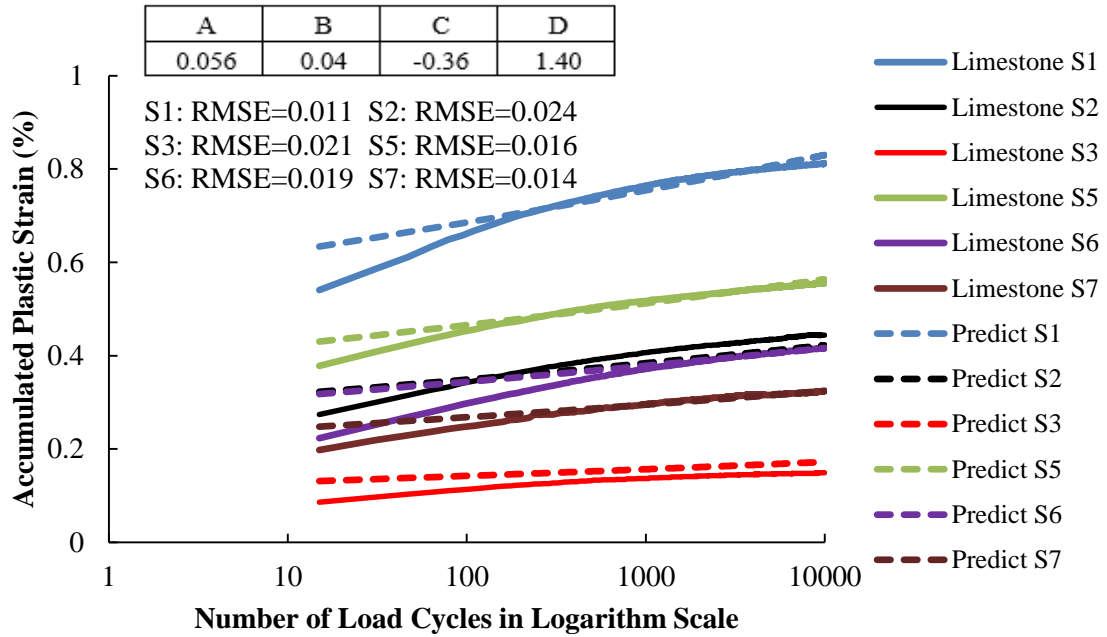


**Figure 19 UIUC model versus measured PD curves for limestone aggregate**

It is shown in Figure 14 and Figure 17 that the MEPDG model significantly underestimates the PD for most of the stress states and in Figure 15 and Figure 18 that the K-T model poorly captures the trend of PD curves for all of the stress states. The K-T model and UIUC also fail to capture the decrease in rate of accumulation of PD at high load cycles due to the direct exponent on the number of load cycles without the natural logarithmic function. The UIUC model cannot accurately capture the trend of PD curves in the first 1,000 load cycles, but fits well with the PD curves in the rest of the load cycles. Another problem existing in the UIUC model is that the coefficient C is determined as a negative value shown in Figure 16 and Figure 19, which is contrary to the fact that a higher deviatoric stress yields a higher PD. The reason for this problem is

that both the deviatoric stress and the shear strength ratio (SSR) are softening terms, and the two terms interfere with each other during the model coefficient regression, which further indicates that the softening and hardening behavior of the UGM are not well characterized in the UIUC model. Due to the determined negative values for the coefficient  $C$ , the UIUC model cannot be used to predict the PD in the hydrostatic stress state, which has a zero deviatoric shear stress. Compared to the UIUC model, the MER model has smaller RMSEs for both the granite aggregates and limestone aggregates, which indicates the proposed model matches much better with the measured PD curves for all of the load cycles.

Using the model coefficients determined in the RLT tests, the various models were used to predict the PD associated with the validation stress states as shown in Table 2. Figure 20 and Figure 21 compare the measured PD curves with the predictions from the K-T, UIUC and MEPDG models with the predictions of the proposed MER model. The determined RMSE values of these three models are higher than those of the MER model for both stress states 8 and 9. This indicates that the proposed model is the best one to predict the rutting behavior of UGMs among these models. It can be seen that at stress state 8 which is outside of the calibration range, both the MEPDG and K-T models were very poor at predicting the PD accurately. This shows the need for models which can handle a wide range of stress states so that improved pavement analysis techniques such as finite element can be used to provide a more detailed design which considers the varied loading regimes of pavements.

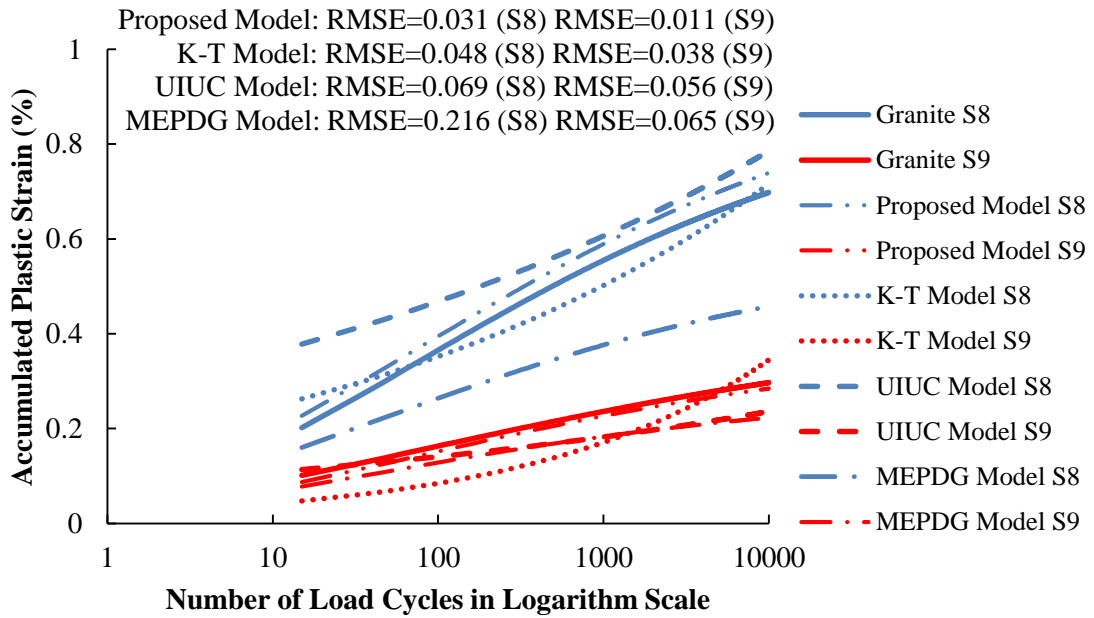


**Figure 20 Comparison of existing model accuracy at validation stress states for granite aggregate**

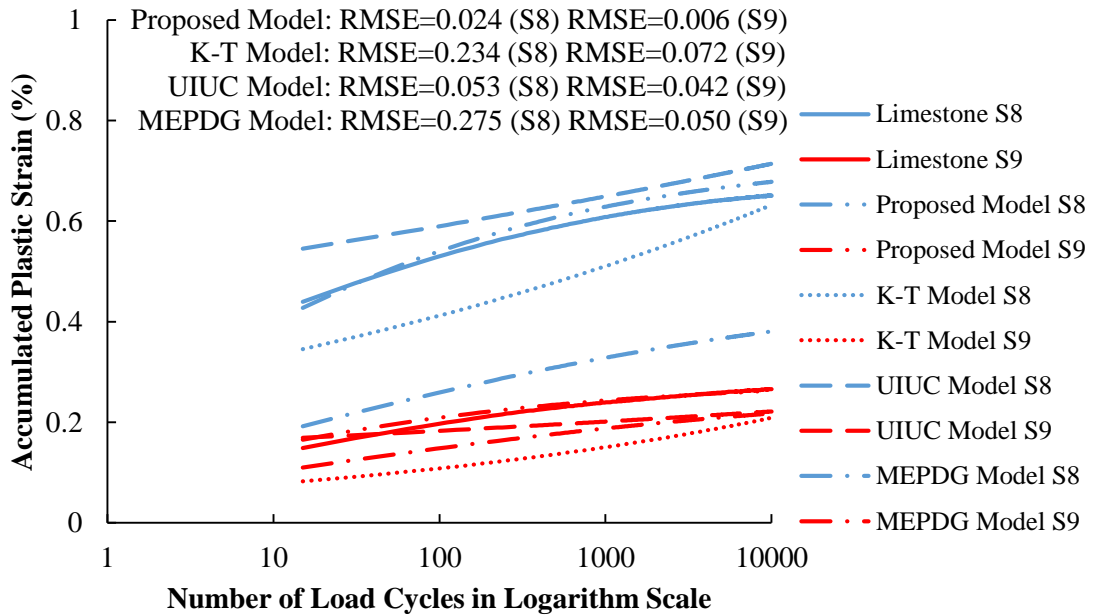


**Figure 21 Comparison of existing model accuracy at validation stress states for limestone aggregate**

## 8. SUMMARY AND CONCLUSIONS

This study proposed a new mechanistic-empirical rutting model to estimate the contribution of unbound aggregate base course to pavement rutting. The new model considers the stress dependency of the rutting behavior by incorporating hardening and softening stress terms into the Tseng-Lytton model. This modification is based on the concept of the Drucker-Prager failure criterion which considers the bulk stress as a hardening term and the deviatoric stress as a softening term. It was demonstrated that the  $I_1$  and  $J_2$  terms clearly affect the hardening and softening effects of stress on the unbound aggregate. It was also observed that the model accurately captured the effects of sample dilation through the re-arrangement of aggregate particles within the matrix as the interparticle stresses were overcome during the testing, resulting in a volumetric reduction in the sample. The permanent deformation, being a result of the volumetric change, is only accurately predicted when the  $I_1$  and  $J_2$  terms are considered.

The MEPDG model in widespread use has been shown to have been surpassed by most of the recently developed models due to the stress dependent nature of aggregates. Laboratory-measured and model-predicted accumulated permanent strain curves are compared in this study. It is shown that the K-T model cannot capture the trend of PD behavior when stress states vary, and the MEPDG model generally underestimates the PD behavior of the tested materials for most of the stress states. The UIUC model fails to capture the trend of PD curves in the first 1,000 load cycles, but is able to fit the PD curves in the rest of load cycles. The proposed MER model accurately



predicts the PD behavior of unbound aggregates throughout the loading stages. The prediction accuracy of the new model is validated by comparing the predicted with the laboratory-measured permanent strain curves at different stress states other than that used for model coefficient calibration. Compared to the K-T model, MEPDG model and UIUC model, the proposed model is capable of accurately characterizing the stress-dependence of the rutting behavior for unbound aggregate materials with only one set of model parameters.

Future work is needed to develop finite element modeling to get the stress state parameters to be used in design of pavement structures. The current linear and non-linear elastic solutions are not adequate to handle the anisotropy and provide the stress dependent properties of unbound base courses. At such time that the stress envelope of pavements can be effectively computed, these improved PD models will be required in order to create first class, effective, and efficient pavements.

## REFERENCES

AASHTO T-307-12, (2012) “Standard Test Method of Test for Determining the Resilient Modulus of Soils and Aggregate Materials”, American Association of State and Highway Transportation Officials, Washington, DC.

Adu-Osei, A., Little, D. N., and Lytton, R. L. (2001). “Cross-anisotropic characterization of unbound granular materials.” *Transportation Research Record: Journal of the Transportation Research Board*, No. 1757, 82-91.

ARA, Inc., ERES Consultants Division. (2004). “Guide for Mechanistic-Empirical Design of New and Rehabilitated Pavement Structures.” NCHRP 1-37A Final Report, Transportation Research Board, National Research Council, Washington, DC.

ASTM D1557-12, (2012) Standard Test Methods for Laboratory Compaction Characteristics of Soil Using Modified Effort (56,000 ft-lbf/ft<sup>3</sup> (2,700 kN-m/m<sup>3</sup>)), American Society for Testing and Materials (ASTM), West Conshohocken, Pennsylvania.

Ayres, M., & Witczak, M. W. (1998). AYMA: Mechanistic probabilistic system to evaluate flexible pavement performance. *Transportation Research Record: Journal of the Transportation Research Board*, 1629(1), 137-148.

Chazallon, C., Hornyh, P., and Mouhoubi, S. (2006). "Elastoplastic model for the long-term behavior modeling of unbound granular materials in flexible pavements."

*International Journal of Geomechanics*, Vol. 6, No. 4, 279-289.

Chen, C., Ge, L., and Zhang, J. (2010). "Modeling permanent deformation of unbound granular materials under repeated loads." *International Journal of Geomechanics*, Vol. 10, No. 6, 236-241.

Chow, L., Mishra, D., and Tutumluer, E. (2014). "Framework for development of an improved unbound aggregate base rutting model for mechanistic-empirical pavement design." *Transportation Research Record: Journal of the Transportation Research Board*, No. 2401, 11-21.

Chow, L. (2014). "Permanent deformation behavior of unbound granular materials and rutting model development." Master Thesis, University of Illinois at Urbana-Champaign, Urbana, Illinois.

Desai, C.S. (1980). "A general basis for yield, failure and potential function in plasticity." *International Journal of Numerical and Analytical Methods in Geomechanics*, Vol. 4, 361-375.

Desai, C.S., and Faruque, M.O. (1984). "Constitutive model for geologic materials." *Journal of the Engineering Mechanics Division*, ASCE, Vol. 110, No. 9, 1391-1408.

Drucker, D.C., and Prager, W. (1952). "Soil mechanics and plastic analysis for limit design." *Quarterly of Applied Mathematics*, Vol. 10, No. 2, 157-165.

Epps, J., Sebesta, S., Hewes, B., Sahin, H., Luo, R., Button, J., Lytton, R., Herrera, C., Hatcher, R., and Gu, F. (2014). "Development of a specification for flexible base construction." Final Report, No. FHWA/TX-13/0-6621, 414pp.

Erlingsson, S., and Rahman, M. (2013). "Evaluation of permanent deformation characteristics of unbound granular materials by means of multistage repeated-load triaxial tests." *Transportation Research Record: Journal of the Transportation Research Board*, No. 2369, 11-19.

Gabr, A., and Cameron, D. (2013) "Permanent strain modeling of recycled concrete aggregate for unbound pavement construction." *Journal of Materials in Civil Engineering*, Vol. 25, No. 10, 1394-1402.

Gu, F., Sahin, H., Luo, X., Luo, R., and Lytton, R. L. (2014). "Estimation of resilient modulus of unbound aggregates using performance-related base course properties." *Journal of Materials in Civil Engineering*, 04014188.

Kenis, W.J. (1978). "Predictive design procedures, VESYS user's manual." Final Report, No. FHWA-RD-77-154, Federal Highway Administration, Mclean, VA.

Kenis, W. J., and Wang, W. (1997). Calibrating mechanistic flexible pavement rutting models from full scale accelerated tests. In *Eighth International Conference on Asphalt Pavements* (Volume I).

Korkiala-Tanttu, L. (2009). "Verification of rutting calculation for unbound road materials." *Proceedings of the Institution of Civil Engineers, Transport* 162, 162(TR2), 107-114.

Lekarp, F., Isacsson, U., and Dawson, A. (2000). "State of the art. II: Permanent strain response of unbound aggregates." *Journal of Transportation Engineering*, Vol. 126, No. 1, 76-83.

Matsuoka, H., and Nakai, T. (1985). "Relationship among Tresca, Mises, Mohr-Coulomb and Matsuoka-Nakai failure criterion." *Soils and Foundations*, Vol. 25, No. 4, 123-128.

Theyse, H. L. (2002). "Stiffness, strength, and performance of unbound aggregate materials: Application of South African HVS and laboratory results to California flexible pavements." *Technical Report*, University of California Pavement Research Center, 86pp.

Tseng, K. H., and Lytton, R. L. (1989). "Prediction of permanent deformation in flexible pavements materials, implication of aggregates in the design, construction, and performance of flexible pavements." ASTM STP 1016, American Society for Testing and Materials (ASTM), pp. 154-172, West Conshohocken, Pennsylvania.

Tutumluer, E. (2013). "Practices for unbound aggregate pavement layers." NCHRP Synthesis 445, TRB, National Research Council, Washington, D.C.

TxDOT TEX-113-E (2011), “Test Procedure for Laboratory Compaction Characteristics and Moisture Density Relationship of Base Materials” Texas Department of Transportation, Austin, TX.

TxDOT TEX-117-E (2010), “Test Procedure for Triaxial Compression for Disturbed Soils and Base Materials”, Texas Department of Transportation, Austin, Texas.

Uzan, J. (1999). “Permanent deformation of a granular base material.” *Transportation Research Record: Journal of the Transportation Research Board*, No. 1673, Transportation Research Board, Washington, D.C., 89-94.

Vermeer, P.A. (1982). “A five-constant model unifying well-established concepts.” *Proceedings of International Workshop on Constitutive Relations for Soils*, Grenoble, France, 175-197.

Witczak, M., & El-Basyouny, M. M. (2004). Calibration of Permanent Deformation Models for Flexible Pavements. *Guide for Mechanistic–Empirical Design of New and Rehabilitated Pavement Structures*. NCHRP 1-37A Appendix GG, Transportation Research Board, National Research Council, Washington, DC.

Xiao, Y., Tutumluer, E., and Mishra, D. (2015). “Performance evaluations of unbound aggregate permanent deformation models for different aggregate physical properties.” *Transportation Research Record: Journal of the Transportation Research Board*, in press.

Zhang, Y., Bernhardt, M., Biscontin, G., Luo, R., and Lytton, R. L. (2014). “A generalized Drucker-Prager viscoplastic yield surface model for asphalt concrete.” *Materials and Structures*, in press.